Liquid Crystals
Publication details, including instructions for authors and subscription information:
http://www.informaworld.com/smpp/title~content=t713926090

Invited Lecture. Complexities in the structure of ferroelectric liquid crystal cells The chevron structure and twisted states

Atsuo Fukuda[a]; Yukio Ouchi[a]; Hidehiko Arai[b]; Hideo Takano[c]; Ken Ishikawa[ad]; Hideo Takezoe[a]
[a] Department of Organic and Polymeric Materials, Tokyo Institute of Technology, O-okayama, Tokyo, Japan [b] Japan Atomic Energy Research Institute, Takasaki-shi [c] Yamato-Laboratory IBM Japan, Kanagawa, Japan [d] Department of Applied Physics, University of Tokyo, Tokyo, Japan

To cite this Article Fukuda, Atsuo , Ouchi, Yukio , Arai, Hidehiko , Takano, Hideo , Ishikawa, Ken and Takezoe, Hideo(1989) 'Invited Lecture. Complexities in the structure of ferroelectric liquid crystal cells The chevron structure and twisted states', Liquid Crystals, 5: 4, 1055 — 1073
To link to this Article: DOI: 10.1080/02678298908026410
URL: http://dx.doi.org/10.1080/02678298908026410

LIQUID CRYSTALS, 1989, VOL. 5, NO. 4, 1055–1073

Invited Lecture

Complexities in the structure of ferroelectric liquid crystal cells
The chevron structure and twisted states

by ATSUO FUKUDA, YUKIO OUCHI, †HIDEHIKO ARAI,
‡HIDEO TAKANO, §KEN ISHIKAWA and HIDEO TAKEZOE
Tokyo Institute of Technology, Department of Organic and Polymeric Materials,
O-okayama, Meguro-ku, Tokyo 152, Japan
†Japan Atomic Energy Research Institute, Watanukicho 1233,
Takasaki-shi, Gunma 370-12,
‡Yamato-Laboratory IBM Japan, 1623-14 Shimotsuruma, Yamato-shi,
Kanagawa 242, Japan

To demonstrate the generality of the chevron structure in ferroelectric liquid crystal (FLC) cells, an optical micrograph is presented, which shows a series of defect lines clearly indicating this structure. The generality is understood as a direct manifestation of the smectic layer undulation playing an important role in the S_A–S_C (S_C^*) phase transition. By establishing the relation between chevrons and asymmetric focal conics, both of which have two senses, $\pm z$, the boundaries between them with opposite senses, i.e. so-called zig-zag defects, have been characterized; the $\langle\langle\langle * \rangle\rangle\rangle$ type boundary does not exist as a line but shrinks into a point. The interplay between the chevron structure and the director alignment has been described in detail; in particular, the appearance of unwinding lines in the middle of thick cells, the characterization of internal disclination loops in SSFLC cells, and the law regulating the emission and absorption of internal disclinations by zig-zag defects. With a view to removing zig-zag defects and to increasing the apparent tilt angle, alignment by obliquely evaporated SiO, which may produce cells free from the chevron structure, alignment by rubbing, and three kinds of electric field effects have been assessed. The rubbing may induce a characteristic deformation of the zig-zag defect loop with a teardrop shape as a consequence of reducing the area surrounded by the loop. Finally, further complexities are noted in connection with the polar surface interaction and the material constants which characterize various director and layer deformations.

1. Introduction

Meyer *et al.* [1] opened a new era by discovering ferroelectric liquid crystals and one of the fascinating topics in this era has been hysteresis. Meyer [2] clearly stated in his review article: "... ... ..., in polydomain samples, or very thin ones contained between surfaces with strong alignment anchoring, there can be pinning effects which produce at least partial hysteresis." A proposal [3, 4] to utilize this hysteresis due to pinning effects in displays clarified the concept of bistable switching in surface stabilized ferroelectric liquid crystal (SSFLC) cells. It was based on an idealized naive

§ Present address: Department of Applied Physics, University of Tokyo, Tokyo 113, Japan.

0267–8292/89 $3.00

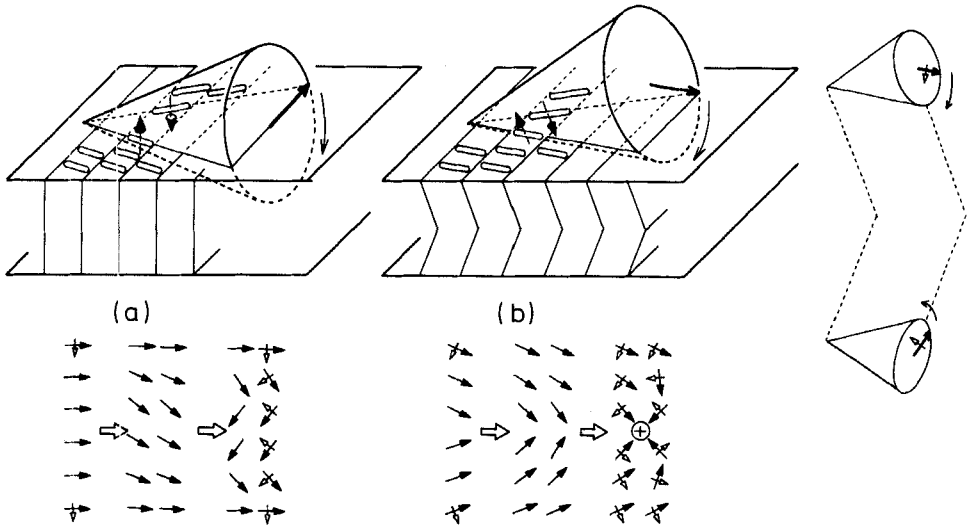

Figure 1. Director motion during bistable switching. (*a*) In an idealized naive structure of SSFLC cells, directors rotate on the cone in the same sense. (*b*) Actually, however, directors rotate on the cone in opposite senses; hence the selective pretilting of the C directors at the top and bottom substrate plates, i.e. the chevron structure of the smectic layers, is necessary.

structure, i.e. the bookshelf structure; the smectic layers are perpendicular to the substrate plates and the molecular long axes are aligned uniformly parallel to the plates in either of the bistable state, as illustrated in figure 1 (*a*). The switching was considered to occur in such a way that all of the molecules rotate on the cone in the same sense [3, 4].

Actually, however, the cell structure and hence the switching process are much more complex. We can appreciate the complexities quite easily, when we observe the switching process by taking stroboscopic photographs using a polarizing optical microscope. Unexpectedly, molecules in the upper half and those in the lower half of the cell rotate on the cone in the opposite sense, as illustrated in figure 1 (*b*) [5–8]. The occurrence of this unexpected molecular motion requires the selective pretilting of C directors at the top and the bottom substrate plates [5–8]. The real cause of the selective pretilting is the smectic layer bending, i.e. the chevron structure [8–14]. In this way, the complexities partly originate from the fact that there exist smectic layers and that they are rather easily deformed.

The directors themselves also deform quite easily and may form helicoidal, twisted (TRr, TRl, TLr, TL1) [5, 6, 8, 15–18] and sometimes deformed (Dr, Dl) [7, 8, 18] states in addition to the uniform states (Ur, Ul). The states actually realized depend not only on extrinsic factors, such as boundary surface conditions and the applied electric field, but also on intrinsic ones such as the elastic constants and powers that produce spontaneous deformations [19–21]. Because of the chevron structure, i.e. the selective pretilting at the bounding surfaces, bistable switching between the optically distinguishable twisted states, Tr and Tl [5, 6, 8, 18, 22, 23], occurs, in addition to the originally proposed bistable switching between the uniform states, Ur and Ul [3, 4]. Actually, many of the FLC displays so far produced as trials appear to utilize the bistability between the two twisted states. As is clearly seen, the boundary between the uniform and the deformed states as well as the boundary between the two twisted states contain internal disclinations [5–8, 17, 18]. Furthermore, during the switching

between the two uniform states, there inevitably appears the internal disclination, in addition to the two surface disclinations on the top and the bottom substrate plates [5–8, 18]. In this way, the chevron structure together with the internal disclination plays an important role.

In §2, we shall report the structural complexities due to the existence of the chevron. Why the chevron structure appears so universally is explained in §2.1, the relation between chevrons and asymmetric focal conics both of which have the two senses, $\pm z$, is clarified in §2.2, and the boundaries between the chevrons or the focal conics with opposite senses, which have been observed by many investigators and called zig-zag defects, are studied in §2.3.

In §3, we shall report the interplay between the chevron structure and the director alignments, in particular, between zig-zag defects and disclinations. The appearance of unwinding lines in the middle of thick cells is discussed in §3.1, internal disclination loops observed in SSFLC cells are characterized in §3.2, and emission and absorption of internal disclinations by zig-zag defects are clarified in §3.3.

In §4, we shall describe possible ways of controlling the layer structure. Alignment by obliquely evaporated SiO, which may produce cells free from the chevron structure but strained slightly, is described in §4.1, alignment by rubbing is assessed in §4.2, and three kinds of electric field effects are considered in §4.3, with a view to removing the zig-zag defects and to increasing the apparent tilt angle. In §5, we shall refer to further complexities and possibilities as a concluding remark.

2. Structural complexities due to chevrons

2.1. *Smectic layer undulation and chevron structure*

We consider first the reason why the chevron structure appears; it is a direct manifestation of elastic fluctuations. Not only the director fluctuation but also the elastic fluctuation, i.e. the smectic layer undulation, plays an important role in the S_A–S_C (S_C^*) phase transition. Note that the undulation is the Nambu–Goldstone mode of the S_A and S_C (S_C^*) phases. Although critical phenomena in the S_A phase have been studied by taking account of the smectic layer undulation [24] using the NAC diagram [25], no one has noticed the direct manifestation of the smectic layer undulation in the S_C (S_C^*) phase before the chevron structure was established experimentally. Suppose that the S_A phase bookshelf structure is formed ideally between two substrate plates set parallel to each other, as shown in figure 2 (*a*); the smectic layers are perpendicular

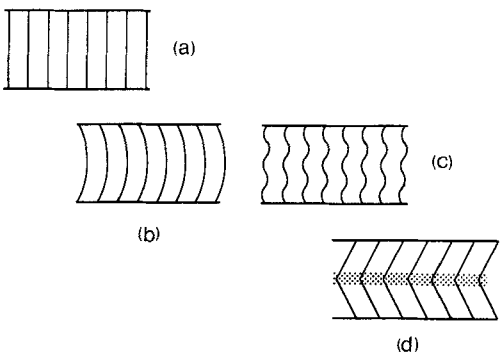

Figure 2. Schematic illustration of the important role played by the smectic layer undulation in forming the chevron structure; (*a*) rigid layers, (*b*) the fundamental mode, (*c*) higher harmonics, and (*d*) the chevron structure. The shaded region in the middle is strained.

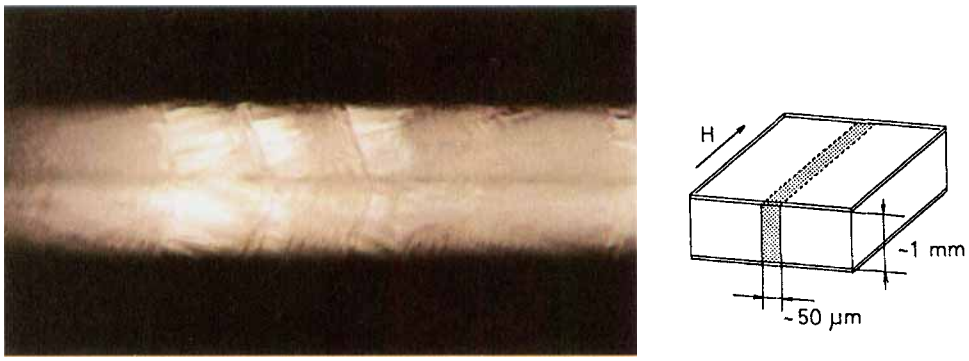

Figure 3. The chevron structure observed by a polarizing optical microscope. The cell used is illustrated.

and hence the directors are parallel to the plates. When the S_A–S_C (S_C^*) phase transition occurs, the smectic layer thickness decreases because of the director tilting from the layer normal. To keep the density constant, either the number of layers or the area of each layer ought to increase. Since the smectic layer undulation is excited, an increase in the area occurs much more easily than the formation of new layers. The molecules attached to either of the substrate plates are difficult to move, so that the fundamental mode of undulation looks something like that shown in figure 2(*b*). However, such a layer deformation is energetically unfavorable, because the layer thickness is not constant. Actually, the chevron structure (*d*) is realized as a superposition of several higher harmonics as shown in (*c*) as well as the fundamental undulation mode (*b*); the layer thickness adapted to the S_C (S_C^*) phase prevails in the whole region except in the thin middle part, as indicated by the shading where the smectic layers bend sharply and are expanded.

Because of its fundamental importance, we have tried to observe the chevron structure with a polarizing optical microscope and one result is shown in figure 3. The cell used is also illustrated in the figure. Its dimension was about 3 mm × 1 mm × 50 μm, and the sample used was CS 1013 (Chisso Petrochemical Corporation). To obtain a single liquid crystal (a monodomain), the cell was cooled from the isotopic to the S_C^* in a magnetic field of about 10 T. Contrary to the ordinary experimental procedure, we have photographed a cross-section of the cell. A series of defect lines clearly indicates the chevron structure, though the details of the defect lines together with their origin have not yet been clarified.

2.2. *Generality of the chevron structure and of the asymmetric focal conics*

As expected from the conclusion derived in §2.1, the chevron structure is observed quite generally in the S_C (S_C^*) phase [12–14]. It appears in cells aligned by several different methods such as a temperature gradient, rubbing, SiO oblique evaporation and a magnetic field, though sometimes surface treatments seriously affect the smectic layer structure so that no chevron is observed [14]. The chevron structure is found in a compound with the phase sequence of N^*–S_C^* so long as the tilt (cone) angle increases with decreasing temperature. The chevron structure is realized in cells as thick as 350 μm where the director forms a helix.

When the cell thickness is large, focal conics may also appear. For simplicity, here we assume an ideal S_A bookshelf structure without any focal conics, though two kinds

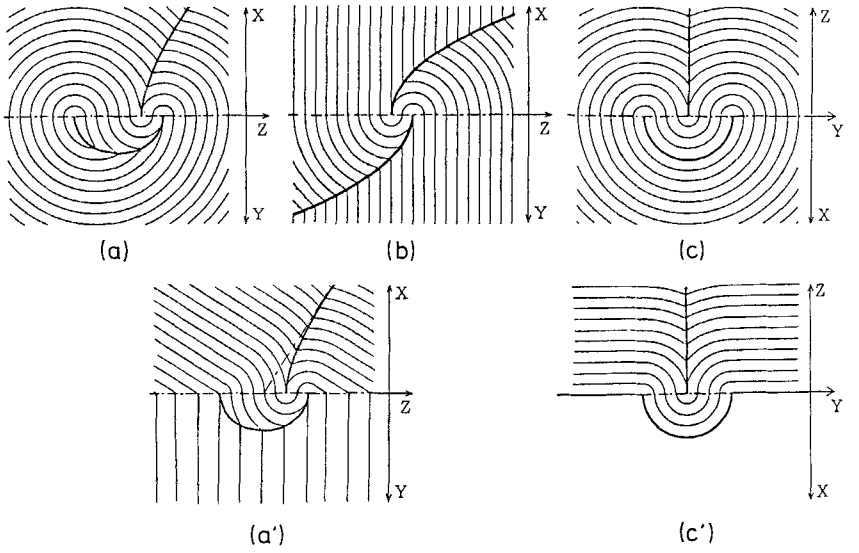

Figure 4. Five types of focal conics are illustrated by drawing two cross-sectional planes containing confocal conics. (*a*), (*b*), and (*c*) are ordinary focal conics; (*b*) and (*c*) can be regarded as special cases of (*a*). (*a'*) and (*c'*) are obtained by opening (*a*) and (*c*) in order to fit in the chevron and bookshelf structures, respectively; asymmetric focal conics (*a'*) can also be regarded as the chevron version of (*b*) and (*c'*). (*a'*) is not a focal conic in the strict sense that the smectic layer spacing is constant everywhere except on the confocal conics.

of focal conics shown in figure 4 (*b*) and (*c'*) are completely compatible with the S_A bookshelf structure [26, 27] and actually the type (*c'*) focal conics is frequently observed as a diamond shaped defect [28]. As the S_A–S_C (S_C^*) phase transition occurs and the smectic layer thickness decreases, the chevron structure is formed. Since the chevron structure has the deformed region as indicated by the shading in figure 2, it may relax to form focal conics.

Contrary to the ideal S_A bookshelf structure, it is impossible to fit a pair of ideal focal conics in the chevron structure; some slight modification is needed. Actually, type (*a'*) asymmetric, slightly deformed focal conics is frequently observed [29], as shown in figure 5. The relation between the chevron structure and asymmetric focal conics is illustrated in figure 6. Ellipses are located in the middle plane of the chevron structure parallel to the substrate plates and perpendicular hyperbolas are observed as bisectors of triangles, which are shadows of elliptical cones with apexes at the intersecting points of the hyperbolas with the substrate plate.

2.3. *Zig-zag defects*

As is clear from figure 6, the chevron tip takes either of the two possible senses, $\pm z$. When the director is parallel to the substrate plates, the two senses are equivalent and the two kinds of chevrons with opposite senses actually appear in a cell. The boundaries between them are known as zig-zag defects. On the analogy of edge and screw dislocations, four simple types of boundaries are, *a priori*, conceivable, as illustrated in figure 7 (*a*). Two of them are parallel and the rest are perpendicular to the smectic layer; the two parallel boundaries correspond to $\langle\langle\langle * \rangle\rangle\rangle$ and $\rangle\rangle\rangle * \langle\langle\langle$,

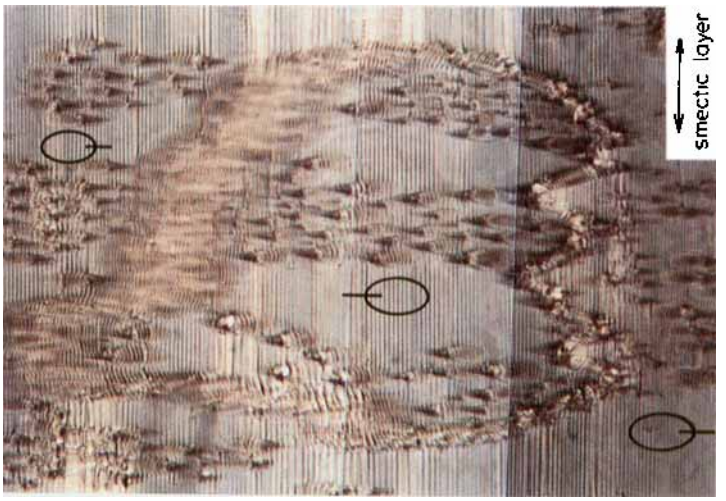

Figure 5. A micrograph showing asymmetric focal conics and a zig-zag defect loop. Inside the loop the asymmetric focal conics point to the left, while outside they point to the right.

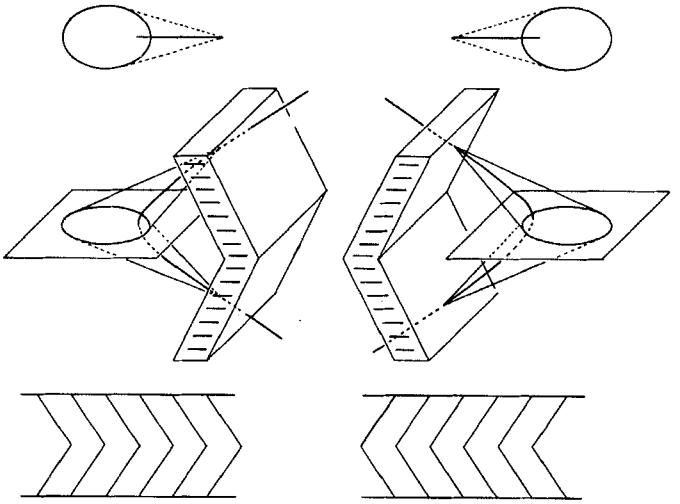

Figure 6. Relation between the chevron structure and the asymmetric focal conics.

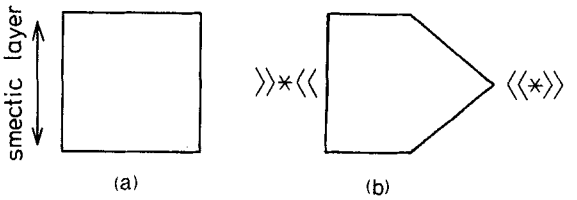

Figure 7. Boundaries between the two kinds of chevrons with opposite senses. (*a*) Similarly to edge and screw dislocations, four simple types are conceivable. (*b*) Actually, however, the ⟨⟨⟨∗⟩⟩⟩ type does not exist as a line but is replaced by oblique lines corresponding to mixed dislocations.

respectively. Actually, however, the zig-zag defects are quite asymmetric along the layer normal direction, as illustrated in figure 7(*b*). The asymmetry indicates a tendency to avoid one type of parallel boundary. Three experimental facts show that the ⟨⟨⟨∗⟩⟩⟩ type does not exist as a line but shrinks into a point (an apex) [29–31]; it is replaced by oblique lines corresponding to mixed dislocations.

Two kinds of models have been proposed for the boundaries; one is the paper folding model [31, 32] and the other is the model with topological singularities [33, 34]. At least when the chevron angle is acute it is natural to consider that the boundaries may contain topological singularities. Then, as illustrated in figure 8, the parallel boundaries are topologically different, though the perpendicular ones are the same. A possible explanation for the tendency to avoid the ⟨⟨⟨∗⟩⟩⟩ type is the difficulty in creating new smectic layers in the middle part of a cell.

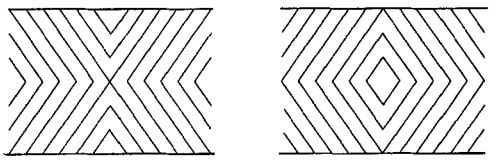

Figure 8. Topological difference between the parallel boundaries, ⟨⟨⟨∗⟩⟩⟩ and ⟩⟩⟩∗⟨⟨⟨.

In addition to this remarkable asymmetry along the layer normal direction, there are indications that the perpendicular boundaries are rather stable and that the ⟩⟩⟩∗⟨⟨⟨ type parallel boundary is always combined with the perpendicular boundaries. Therefore, conceivable types of turns that zig-zag defect lines make are summarized as shown in figure 9. Because types (*d*) and (*e*) are not frequently observed, the zig-zag defect lines are considered to consist of two parts; the lightning part has apexes formed with thin lines oblique to the smectic layer, while the hairpin part consists of thick lines parallel to the layer together with thin lines along the layer normal. The hairpin part is easily curved, but the lightning part is always rather straight. The lightning and hairpin parts of lines may run separately from edge to edge of a cell. Both of them may often be combined to form defect loops with a teardrop or bear paw shape [32]. Although the lightning part appears to be transformed continuously to the hairpin part or vice versa, the properties change rather critically as will be explained later in connection with the domain nucleation during the switching process [32].

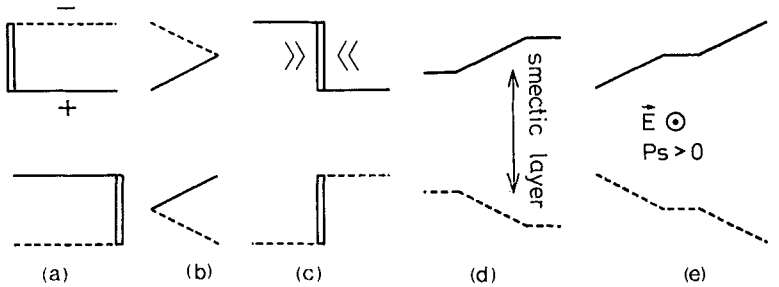

Figure 9. Types of turns that zig-zag defect lines make. Double lines are the ⟩⟩⟩∗⟨⟨⟨ boundaries, and solid and dotted lines are the perpendicular boundaries containing the $\pm 2\pi$ wedge disclination components, respectively. The sign does change in (*a*) and (*b*), while it does not change in (*c*), (*d*), and (*e*). See figure (12).

The zig-zag defects are arranged in a very characteristic way because of their inherent properties. When observed along the smectic layer normal, the harpin and the lightning parts appear alternately. The defect loops with a tear-drop or bear paw shape face toward the same sense unless they are separated by another zig-zag line [32].

As was explained in §2.2, the focal conics produced after the S_A–S_C (S_C^*) phase transition are quite asymmetric along the layer normal direction and hence take either of two possible senses, $\pm z$, as do the chevron tips. Figure 5 also shows that they appear to coalesce and to form defect lines, which are exactly like the zig-zag defects [29]. The detailed coalescence processes and the resultant structures have not yet been clarified, but in figure 5 at least two structures corresponding to the hairpin and lightning parts are clearly distinguishable. The focal conics face toward the same sense unless they are separated by a zig-zag defect. Since the asymmetric focal conics clearly indicate the chevron tip senses, as illustrated in figure 6, it is safe to conclude that the $\langle\langle\langle * \rangle\rangle\rangle$ type parallel boundaries are avoided and only exist as the apexes of the lightning part.

3. Interplay between the chevron structure and director alignment

3.1. *Unwinding lines and chevrons*

When the directors form a helix, a series of the twist disclination lines called dechiralization lines or unwinding lines appear to reconcile the helical structure with the director alignment on the substrate plates [35, 36]. Pavel presented two kinds of models consisting of twist disclination pairs near the substrate plate, one with the directors tilted in the same sense at the top and bottom plates and the other with the directors tilted in the opposite senses [37].

However, during the study of phenomena that depend on the helical pitch and spontaneous polarization in FLCs using mixtures of active DOBAMBC with its racemate, Tsuchiya *et al.* noticed that a series of unwinding lines existed not only near the substrate plates but also in the middle of a cell [38]. There is a pair of $\pm 2\pi$ twist disclination lines per full pitch in the middle, and one $+2\pi$ (-2π) twist disclination line per full pitch near the top (bottom) substrate plate. Martinot-Lagarde also observed a series of unwinding lines other than those near the substrate plates [38]. A delicate energy balance was considered to be responsible for the appearance of the series of disclination lines, but nobody was successful, at that time, in explaining why there appear unwinding lines in the middle.

On the basis of the chevron structure, the appearance of the unwinding lines in the middle is quite understandable. An example is given in figure 10, where one zig-zag defect of teardrop shape is observed, in addition to several focal conics. Inside the zig-zag defect the chevron tip is directed toward the left, while outside it is oriented toward the right. Since the sample is CS 1013 (Chisso Petrochemical Corporation) and the cell is 50 μm thick, the helix is partially unwound and a region appears where no unwinding lines are observed; the directors on the top and bottom substrate plates are tilted in the opposite senses. At least two kinds of fringes are noticed; one is thick and red or green coloured, while the other is thin. Two pairs of twist disclination lines located both in the upper and lower halves and nearly overlapped with each other give rise to the coloured thick fringe, while the thin fringe consists of a pair of twist disclinations in either the upper or the lower half.

The existence of the twist disclination lines in the middle was clearly confirmed by changing the focusing plane from the top to the bottom substrate plate and taking micrographs. The chevron tip senses are determined as illustrated using figure 6. The cross-sectional arrangement of disclination loops depends on the chevron angle, the

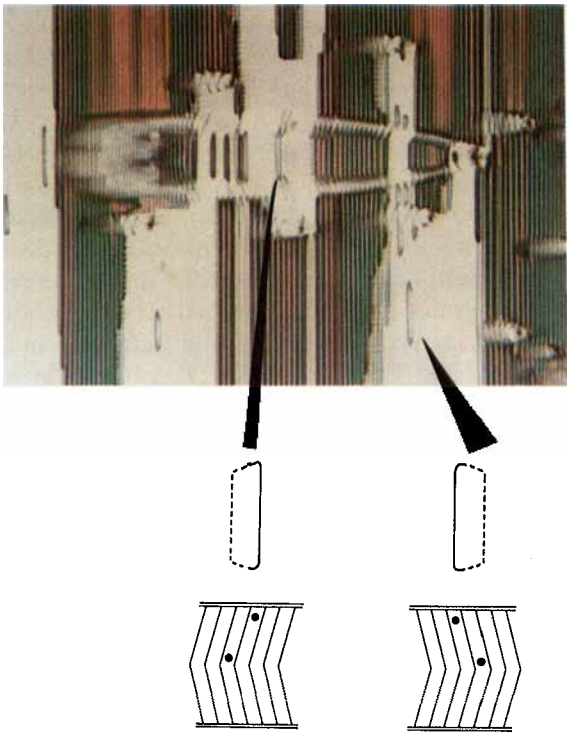

Figure 10. A micrograph showing unwinding lines and a zig-zag defect loop together with focal conics. The cross sections of the unwinding lines are also illustrated schematically.

helical pitch† and handedness, and the director alignment in the middle plane containing the chevron tips as well as on the bounding surfaces. Because its details have not yet been studied, only a schematic drawing is shown in figure 10. Actually, much information is contained in the pattern of the disclination lines. The pattern is very useful to understand the detailed structure of the zig-zag defects as well as the asymmetric focal conics; note, for example, a helical disclination line curled around a focal conics. Brunet‡ has also observed several loops located equidistantly as well as helices around zig-zag defects. A real problem that remains is the director alignment near the chevron tips in the middle of a cell, where the smectic layers are highly strained. The strain may affect the unwinding lines; it appears to be responsible for the fact that the unwinding lines in the middle frequently become dotted as shown in figure 10.

3.2. *Internal disclination loops and chevrons*

We now consider the surface stabilized states where the helix is unwound, explaining that the twisted state has net upward or downward spontaneous polarization because of the chevron structure. The two twisted states, TR and TL, differing in the

† Because of the chevron structure, the helical axis is not parallel to the substrate plates. To obtain the helical pitch, the separation between the neighbouring unwinding lines near a bounding surface should be divided by cos δ, where δ is the angle between the smectic layer normal and the substrate plate.

‡ Brunet, M. (private communication); one of the authors (AF) would like to thank her for showing him the elegant micrographs.

twist sense, right or left, can be recognized using a polarizing optical microscope [5, 15, 16]. The polar surface interaction and the spontaneous C director bending power together with some other material constants may stabilize either TR or TL. Both TR and TL have two substates, T1 and T2, which were classified by the rotation sense of the C directors [5, 17].

Combining this simple model with the chevron structure, the selective pretilting of the C directors on the substrate plates is naturally introduced if the n directors on the bounding surfaces are assumed to be parallel to the substrate plates [9]. The selective pretilting of C directors endows each twisted state with net upward or downward spontaneous polarization and hence an electric field applied perpendicularly to the substrate plates drives the boundary between the twisted states to move [6]. Thus, one of the twisted states is always related to the uniform state Ur, and the other to Ul; it is reasonable to rename T1 and T2 as Tr and Tl [29]. In the same way, the deformed states are also correlated with the uniform states and are named Dr and Dl [29].

Hiji *et al.* were successful in explaining that the two twisted substates, Tr and Tl, give different optical transmission spectra and that the spectra interchange with each other upon rotating a cell by the apparent cone angle [22, 23]. Because of the chevron structure, there are four twisted substates Tr+, Tl+, Tr− and Tl−, where ± indicate that the chevron tips orient $\pm z$, respectively. By comparing the colour of the twisted states stabilized by a lateral electric field with the colour calculated by a model described earlier, Hiji *et al.* distinguished all these substates and concluded that the apexes of lightning and the thick lines of hairpin zig-zag defects correspond to ⟨⟨⟨∗⟩⟩⟩ and ⟩⟩⟩∗⟨⟨⟨, respectively [30].

The boundaries between the surface stabilized states are characterized by two surface and one internal disclinations. The surface disclination loops are usually observed as a speckled pattern. On the other hand, the internal disclination loop may frequently appear as the boundary of a single, independent domain of characteristic form [6–9]. Because of the chevron structure, the internal disclination loop is constrained to lie in the middle plane which contains the chevron tips [31]. This fact explains the experimental observation that the internal disclination loops always coalesce smoothly without overlapping at different depths.

A priori, a rectangular loop consisting of $\pm 2\pi$ twist and $\pm 2\pi$ wedge disclinations of C directors is conceivable; $\pm 2\pi$ twist disclinations are topologically the same, but $\pm 2\pi$ wedge disclinations are different [6–9]. Actually, the loop looks like a boat (pentagon) in well aligned cells when the domain growth rate is slow, being asymmetric

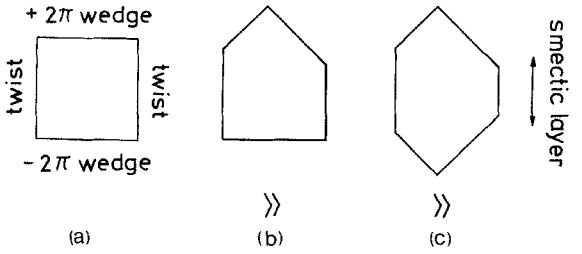

Figure 11. Shapes of internal disclination loops. (*a*) *A priori*, a rectangular loop consisting of the $\pm 2\pi$ twist and the $\pm 2\pi$ wedge disclinations of C directors is conceivable. Actually, however, (*b*) the loop is pentagonal when the domain growth rate is slow, and (*c*) hexagonal when the growth rate is fast. Because of the chevron structure, they are also asymmetric along the smectic layer normal.

along the smectic layer direction, as illustrated in figure 11; when the growth rate is fast, it becomes a hexagon. Now a question arises; which of the bow or the stern corresponds to the $+2\pi$ or -2π wedge disclination? When they determined the absolute configuration of parallel boundaries of zig-zag defects, ⟨⟨⟨*⟩⟩⟩ and ⟩⟩⟩*⟨⟨⟨, Hiji *et al.* also assigned the bow of the boat to the $+2\pi$ disclination and the stern to the -2π disclination [29, 30]. Because of the chevron structure, the observed disclination loop is not strictly symmetric along the smectic layer normal direction, either, as illustrated in figure 11 [29]. The shape of the disclination loop may be calculated using Wullf's theorem of crystal growth [39].

3.3. *Emission and absorption of internal disclinations by zig-zag defects*

The appearance of internal disclination loops is a catastrophic phenomenon and hence their nucleation is liable to occur from any kind of defect. Actually, zig-zag defects frequently nucleate internal disclination loops. For simplicity, we consider the switching between twisted states [32]. Figure 12 illustrates a cross section parallel to the smectic layer which crosses two zig-zag defects at the hairpin part; it is assumed that the material has a positive spontaneous polarization and that the molecular long axes are parallel to the substrate plates [1, 32]. As is clearly seen in the figure, the hairpin part perpendicular to the smectic layer contains either of the $+2\pi$ or -2π wedge disclination of C directors. Similarly, the lightning part contains a mixed disclination, the wedge component of which may be $+2\pi$ or -2π [32]. When we observed the defects along one of the smectic layers, the sign changes alternately. Therefore, the sign changes when the defect turns, as shown in figure 9 (*a*) and (*b*), while it remains the same in the case of (*c*), (*d*), and (*e*). In this way, we can distinguish the $\pm$ hairpin and $\pm$ lightning parts, respectively, according to the sign of the wedge disclination components contained. In a CS 1013 cell of about 4 μm thickness, the + part looks bright and the − part looks dark under crossed Nicols when the polarizer transmitting direction is parallel to the molecular long axis on the bottom substrate plate.

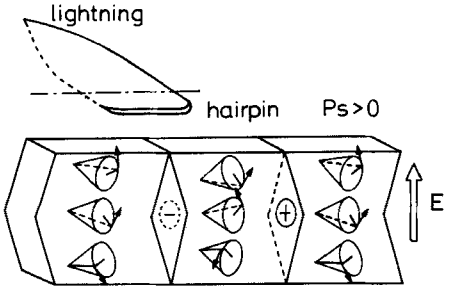

Figure 12. A cross-section parallel to the smectic layer which crosses two zig-zag defects at the hairpin part. The zig-zag defects contain either of the $+2\pi$ or -2π disclination of C directors alternately.

The switching process between Tr and Tl can be described as the emission and the absorption of $\pm 2\pi$ disclinations by zig-zag defects [32]. There is a marked tendency for the hairpin part to hold the -2π disclination while the lightning part holds the $+2\pi$ disclination. The + hairpin part emits the $+2\pi$ mixed disclination, i.e. the bow of the boat, while the − lightning part emits the -2π wedge disclination, i.e. the stern of the boat. After emitting two disclinations on both sides, they change sign.

Figure 13 summarizes the emission and absorption processes of the $\pm 2\pi$ disclinations by the typical zig-zag defect loop.

We now consider the initial stage of disclination emission and absorption inside the zig-zag defect. The zig-zag defect has rather well-defined contours and looks almost uniform in the twisted state. As the applied electric field changes from up to down, the + hairpin part perpendicular to the smectic layer (DE in figure 13) appears to nucleate disclination lines at the contours, as illustrated in figure 14; the nucleation at one of the contours occurs independently of that at the other and hence the disclinations may or may not be emitted on both sides of the zig-zag defect at the same time. The − lightning part (AB), on the other hand, appears to have disclination lines beforehand at both of the contours; these two disclination lines inside the zig-zag defect are emitted on both sides at always almost the same time. In this way, more complicated changes appear to occur before the disclination emission in the + hairpin part than in the − lightning part.

During the disclination absorption process, the + lightning part (EA in figure 13) appears to show more complicated changes after the absorption than the − hairpin part (BC) does. In order to understand the changes inside the zig-zag defect, the detailed defect structure together with that of the chevron itself must be clarified. The

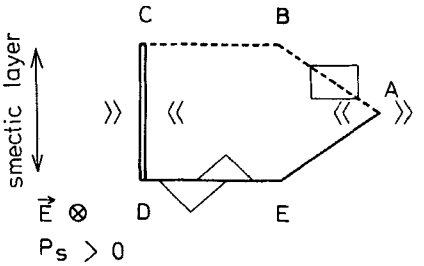

Figure 13. Emission and absorption processes of $\pm 2\pi$ disclinations by a typical zig-zag defect loop during the switching from one twisted state stabilized by the upward field to the other twisted state stabilized by the downward field. The DE part containing the $+2\pi$ wedge disclination under the upward field emits the $+2\pi$ mixed disclination (the bow of the boat), and the *AB* part containing the -2π wedge disclination component under the upward field emits the -2π wedge disclination (the stern).

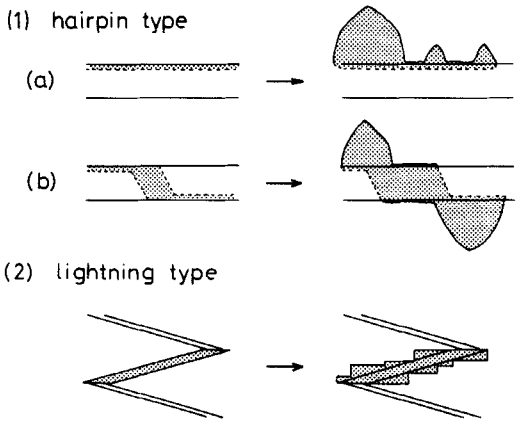

Figure 14. Nucleation of internal disclinations inside zig-zag defects.

study of dichiralization lines as well as the microspectroscopy mentioned in §§3.1 and 3.2 should be useful for this. Observation of the switching process between the uniform states, Ur and Ul, i.e. the interaction of surface disclinations with zig-zag defects, is also important. These are future problems to be studied.

4. Control of smectic layer structure

4.1. *Alignment by obliquely evaporated SiO*

The chevron structure may seriously decrease the apparent tilt angle which is responsible for the contrast of Clark–Lagerwall type FLC displays [3, 4]. Suppose new smectic layers are easily formed and the bookshelf structure in the S_A phase is maintained even in the S_C (S_C^*) phase; then the apparent tilt angle is equal to the real one, as illustrated in figure 15 (*a*). In contrast, if all of the change in the smectic layer thickness is reconciled by the chevron structure, the apparent tilt angle becomes zero, as illustrated in figure 15 (*b*) [12, 14].

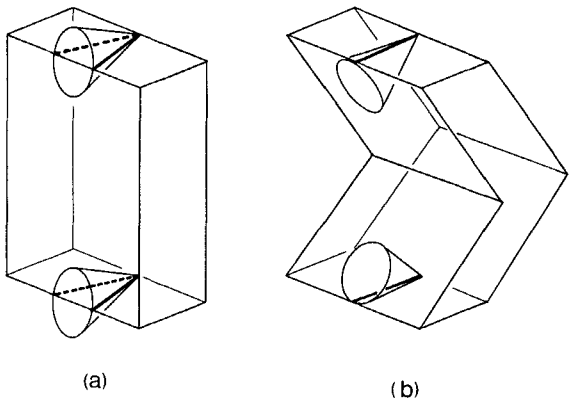

Figure 15. The apparent tilt angle and the smectic layer structure, (*a*) when the bookshelf structure in the S_A phase is maintained even in the S_C (S_C^*) phase, and (*b*) when all of the change in the smectic layer thickness is reconciled by the chevron structure.

The SiO oblique evaporation technique provides a large pretilting in the N (N*) phase; it has been used to control the smectic layer structure by several groups [13, 14, 40–43]. Ouchi *et al.* clearly showed, by X-ray diffraction, that SSFLC cells aligned with the SiO oblique evaporation technique may have either of the two types of smectic layer structures, chevron or uniform tilt, according to the parallel and antiparallel combination of two substrate plates [13, 14]. When SiO is vacuum deposited obliquely at an angle of about 80° on a substrate plate, it forms columns as illustrated in figure 16 [43, 44]. Since the columns are not perpendicular to the plate, two kinds of cells are possible as shown in figures 16 (*a*) and 16 (*b*); these are called

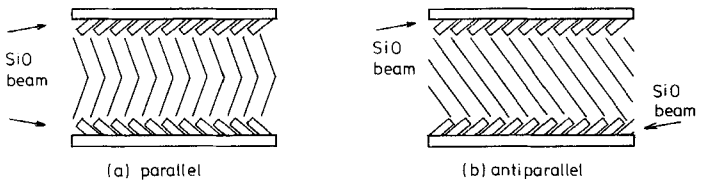

Figure 16. The column directions and the SiO evaporation directions in (*a*) parallel and (*b*) antiparallel cells.

parallel and antiparallel cells, respectively, by noting not the column directions but the SiO evaporation directions.

In the N (N*) phase, the molecular long axes are pretilting approximately parallel to the columns at the bounding surfaces [43, 44]. In the antiparallel cell, therefore, the smectic layers are formed obliquely by keeping the pretilting angle almost constant, at least when the S_A phase is formed via the N (N*) phase. In the parallel cell, on the other hand, the situation is not so simple. The smectic layers formed from the top surface are not parallel to those from the bottom surface, and the chevron structure is observed even in the S_A phase [14]. In order to maintain the pretilting angle in the N (N*) phase, the chevron may become very accute. Actually, however, the chevron is obtuse and the pretilting angle in the S_A phase becomes rather small; the acute chevron appears to increase the free energy remarkably. In any case, the parallel cell is highly strained in the S_A phase; this is consistent with the very broad Bragg reflections.

After the S_A–S_C (S_C^*) transition, the cone angle gradually increases and hence the smectic layer thickness decreases. This decrease may, at least partly, be compensated for by the layer tilting, the chevron or a uniform tilt. Since the tilting sense is uniquely determined in the S_A phase, the boundaries between the two senses $\pm z$, such as the zig-zag defects, are not observed in the S_C (S_C^*) phase [40]. In the parallel cell, the chevron gradually becomes acute, and the pretilting on the bounding surfaces increases, approaching the value in the N (N*) phase; the sharp layer bending at the chevron tip appears to occur more easily in the S_C (S_C^*) phase than in the S_A phase. The increased pretilting decreases the strain produced in the S_A phase, and the width of the Bragg reflection in the S_C (S_C^*) phase is smaller than that in the S_A phase; at the same time, however, the apparent tilt angle is much smaller than the real one.

The uniform tilt angle in the antiparallel cell also increases in the S_C (S_C^*) phase. Since the molecules on the bounding surfaces hardly move, an increase in the layer tilt angle could not easily occur and might induce additional strain, causing a broader Bragg reflection. Actually, an increase of the layer tilt angle in the antiparallel cells is much smaller than that in the parallel cells, and the apparent tilt angle becomes relatively large as compared to that in the parallel cell. However, the width of the Bragg reflection also decreases in the S_C (S_C^*) phase. The reason is not clear at present and we are in the process of detailed studies.

4.2. *Alignment with high pretilting by rubbing*

As is clearly indicated by the X-ray study of cells with obliquely evaporated SiO, alignment with high pretilting by rubbing is effective in controlling the smectic layer structure and in obtaining cells free from zig-zag defects; the alignment may also be helpful in increasing the apparent tilt angle. Important factors are the pretilting angle, the off-plane and on-plane anchoring strength, and the hindrance of layer movement at the bounding surfaces. Ordinary alignment with no or low pretilting by rubbing appear to produce the chevron structure which absorbs almost all of the change in the smectic layer thickness.

It is worthwhile noting the following two facts. One is the definition of the true tilt angle θ and the other is the fact that the apparent tilt angle is very sensitive to the angle $\delta = \delta_C - \delta_A$ when $\delta_A \sim 0$ and δ is close to its maximum value θ. Here δ_A and δ_C are the observed layer tilt angles on the bounding surfaces in the S_A and S_C phases, respectively, and 2θ is the true cone angle. The true tilt angle is defined as the angle between the smectic layer normal and the molecular long axis; the problem is how to determine the molecular long axis. Both the X-ray method [45] and the optical one

[46] has been used and it is known that the axes thus obtained do not always coincide with each other. Here, however, we disregard this difference for the sake of simplicity.

As in the case of obliquely evaporated SiO, two kinds of cells, parallel and antiparallel, are distinguishable by noting the rubbing directions of two substrate plates. In the parallel cell, zig-zag defects may not appear when the pretilting is suitably high and the off-plane anchoring is strong enough. Even when these conditions are not fully satisfied, the ⟨⟨⟨ chevron is, in principle, not equivalent to its ⟩⟩⟩ counterpart and this non-equivalence is observed as a difference in area. An example is given in figure 17. The sample, CS 1013 (Chisso Petrochemical Corporation), was aligned by rubbing a polyvinyl alcohol film coated on the substrate plates; the cell thickness was 3 μm. The rubbing direction is indicated by arrows. Note that the area surrounded by zig-zag defect loops where the smectic layers are deformed like ⟨⟨⟨ is much smaller than the remaining area with the ⟩⟩⟩ chevron structure. The micrograph shown is not a special part of the cell and the difference in area is observed throughout the cell. In this way, we conclude that the rubbing induces the pretilting at the bounding surfaces and favours the ⟩⟩⟩ chevron structure.

The tendency to reduce the area surrounded by zig-zag defect loops deforms the hairpin part significantly. A glance at the zig-zag defect loops may not allow the difference between the hairpin and lightning parts to be found. By observing the

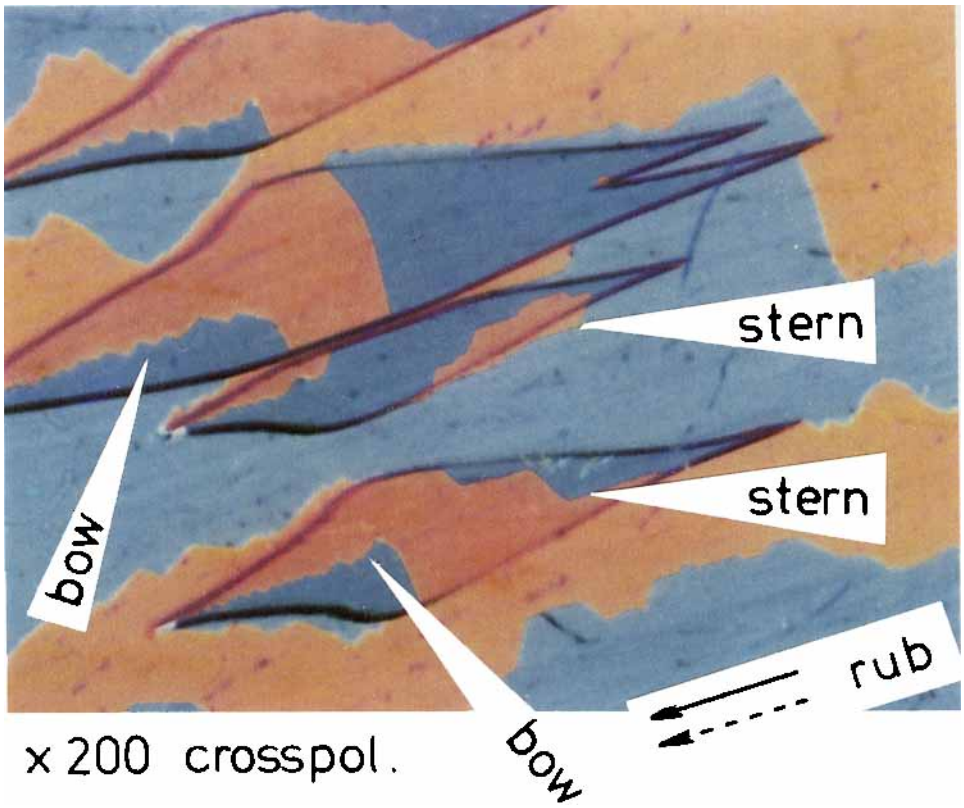

Figure 17. A micrograph of a parallel cell (CS 1013, 3 μm in thickness) aligned by rubbing polyvinyl alcohol film coated on the substrate plates. Arrows indicate the rubbing directions on the top and the bottom substrate plate.

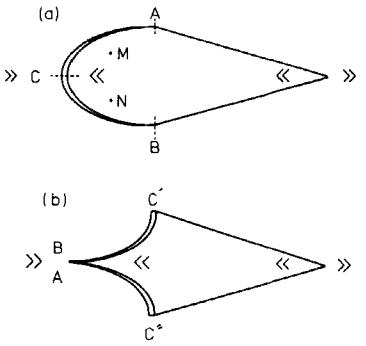

Figure 18. A possible explanation for the deformation of a zig-zag defect loop with a teardrop shape. By 180° rotation about the normal axes M and N, the AC and BC parts in (*a*) change into the C′A and C″B parts in (*b*).

emission process of boat shaped disclination loops during switching between the bistable twisted states, however, they can be distinguished clearly, as indicated in figure 17. A possible explanation for the deformation in the hairpin part is as follows. Because the hairpin part is liable to deform, a typical zig-zag loop with a pentagonal shape may become a loop with a tear drop shape as shown in figure 18 (*a*). Let us cut it at three points, *A*, *B*, and *C*, and replace the *AC* and *BC* parts as indicated in figure 18 (*b*). Note that, because of symmetry, the properties of the boundary in figure 18 (*b*) is almost the same as those in figure 18 (*a*) except for the points *A*, *B*, and *C*, and that the surrounded area in figure 18 (*b*) is clearly reduced considerably.

4.3. *Effects of an electric field*

At least three kinds of effects are conceivable. The first is the electroclinic effect observed in the S_A phase, and the second is the effect which may accompany the smectic layer deformation in the S_C^* phase. When the S_A phase does not appear and the S_C^* phase is formed directly from the N* or isotropic phase, several equivalent directions frequently exist along which the smectic layers grow and the third effect may be observed; the application of an electric field during the phase transition is effective in choosing one of these directions. In the temperature gradient method [47], for example, which is used to prepare SSFLC cells, the molecular long axes are forced to be parallel to a spacer edge as well as to the substrate plates. When the S_A phase is formed, the direction of the smectic layers is uniquely determined perpendicular to the spacer edge and to the substrate plates. When the S_C^* phase is formed directly from the isotropic or N* phase, however, two kinds of smectic layers nucleate from the spacer edge even if they are assumed to be perpendicular to the substrate plates. Because the spontaneous polarization is parallel to the smectic layer and perpendicular to the tilting plane spanned by the molecular long axis and the smectic layer normal, an electric field applied perpendicular to the substrate plates may determine the smectic layer direction uniquely [48].

In the chevron structure, the spontaneous polarization is not perpendicular to the substrate plates because of its characteristic direction. Hence an electric field applied perpendicular to the substrate plates exerts a force on the smectic layers so as to take the bookshelf structure. Ouchi *et al.* confirmed such a change in the smectic layer structure by carefully observing the switching process [9]; Sato *et al.* also reported a

similar change [49]. The force exerted sometimes causes zig-zag defects to move. This movement is very sensitive to the strength and frequency of an applied field; when they are suitable, the defects may disappear almost completely though the chevron structure itself appears to remain.

An electroclinic effect in the chiral S_A phase is a kind of inverse piezoelectric effect in crystalline phases; a molecular tilt angle θ relative to the smectic layer normal is induced by applying an electric field parallel to the layer. This effect was first observed by Garoff and Meyer [50] and was investigated as an inconspicuous pretransitional phenomenon [51]. Recently, however, a wide variety of ferroelectric liquid crystals with large spontaneous polarization have been synthesized because of their potential application to display devices; in such materials, the electroclinic effect is conspicuous and a tilt angle as large as 10° is induced by a field of about 10 V/μm at temperatures above $T_{S_C^*S_A}$ by several degrees or more [52–54].

The detailed process of inducing the tilt angle may consist of at least three movements. The applied electric field hinders the free rotation of molecules around their long axes and aligns the dipole moments to some extent, the resulting polarization tilts the molecular long axes, and the tilted director causes the smectic layer deformation. The chevron structure appears to be formed, since some zig-zag defects, though vague, were observed [29]. Moreover, normalized temporal changes of light transmittance due to the electroclinic effect are independent of the applied field strength and are described by an exponential curve composed of at least two components [55]. The slow component appears to be related to some smectic layer deformation. We are in the process of making a detailed study of this.

5. Further complexities

Complexities in structure of ordinary SSFLC cells result from the chevron structure as well as the twisted states. Here we have been trying mainly to clarify the chevron structure and to study the possibility of controlling the smectic layer structure. In order to realize the bistable switching between the uniform states ideally, however, we also have to suppress the twisted states. For this purpose, we need to understand the polar surface interaction and the material constants that characterize various director and layer deformations, spontaneous and forced. A variety of material constants add further complexities and possibilities. At least two novel switching processes have been reported, which appear to be related with the fact that some of the material constants have extraordinary values. One is the bistable switching between the uniform states via the helical state [56], and the other is the tristable switching in SSFLC cells [57]. We would like to clarify these complexities from an optimistic point of view, hoping to realize FLC displays in the near future.

The authors' grateful thanks are due to Dr S. Shimamoto for the use of a superconducting magnet of the Naka Establishment of JAERI and to Drs T. Ando and M. Nishi for able collaboration in the superconducting magnet experiment. The authors also express thanks to Dr S. Machi, Director of the Department of Research of JAERI for his support of this study and to Dr I. Kuriyama, Director of Takasaki Branch of Irradiation Development Association for suggesting the experiments using a superconducting magnet.

References

[1] MEYER, R. B., LIEBERT, L., STRZELECKI, L., and KELLER, P., 1975, *J. Phys., Paris*, **36**, L69.
[2] MEYER, R. B., 1977, *Molec. Crystals liq. Crystals*, **40**, 33.

[3] CLARK, N. A., and LAGERWALL, S. T., 1980, *Appl. Phys. Lett.*, **36**, 899.
[4] CLARK, N. A., HANDSCHY, M. A., and LAGERWALL, S. T., 1983, *Molec. Crystals liq. Crystals*, **94**, 213.
[5] ISHIKAWA, K., OUCHI, Y., UEMURA, T., TSUCHIYA, T., TAKEZOE, H., and FUKUDA, A., 1985, *Molec. Crystals liq. Crystals*, **122**, 175 (*Proc. 10th Int. Liq. Cryst. Conf.* (York, 1984)).
[6] ISHIKAWA, K., UEMURA, T., TAKEZOE, H., and FUKUDA, A., 1985, *Jap. J. appl. Phys.*, **24**, L230.
[7] OUCHI, Y., ISHIKAWA, K., TAKEZOE, H., FUKUDA, A., KONDO, K., ERA, S., and MUKOH, A., 1985, *Jap. J. appl. Phys.*, **24**, Suppl. 24–2, 899 (Proc. 6th Int. Meeting on Ferroelectricity (Kobe, 1985)).
[8] OUCHI, Y., TAKEZOE, H., and FUKUDA, A., 1987, *Jap. J. appl. Phys.*, **26**, 1.
[9] OUCHI, Y., TAKANO, H., TAKEZOE, H., and FUKUDA, A., 1987, *Jap. J. appl. Phys.*, **26**, L21.
[10] RIEKER, T. P., CLARK, N. A., PARMAR, D. S., SMITH, G., and SAFINYA, C. R., 1986, *Abst. 11th Int. Liq. Cryst. Conf.* (Berkeley, 1986) Θ-042-FE.
[11] CLARK, N. A., and LAGERWALL, S. T., 1986, *Japan Display '86* (*Proc. 6th Int. Display Research Conf.* (Tokyo, 1986)) 12.1-Invited, p. 456.
[12] RIEKER, T. P., CLARK, N. A., SMITH, G. S., PARMAR, D. S., SIROTA, E. B., and SAFINYA, C. R., 1987, *Phys. Rev. Lett.*, **59**, 2658.
[13] OUCHI, Y., LEE, J., TAKEZOE, H., FUKUDA, A., KONDO, K., KITAMURA, T., and MUKOH, A., 1988, *Jap. J. appl. Phys.*, **27**, L725.
[14] OUCHI, Y., LEE, J., TAKEZOE, H., FUKUDA, A., KONDO, K., KITAMURA, T., and MUKOH, A., 1988, *Jap. J. appl. Phys.*, **27**, L1993.
[15] HANDSCHY, M. A., CLARK, N. A., and LAGERWALL, S. T., 1983, *Phys. Rev. Lett.*, **51**, 471.
[16] GLOGAROVA, M., and PAVEL, J., 1984, *J. Phys., Paris*, **45**, 142.
[17] LEJCEK, L., GLOGAROVA, M., and PAVEL, J., 1984, *Phys. Stat. Sol.* (*a*) **82**, 47.
[18] OUCHI, Y., TAKEZOE, H., and FUKUDA, A., 1988, *Ferroelectrics*, **85**, 501 (*Proc. 1st Int. Symp. on Ferroelectric Liq. Cryst.* (Bordeaux-Archachon, 1987)).
[19] TSUCHIYA, T., TAKEZOE, H., and FUKUDA, A., 1986, *Jap. J. appl. Phys.*, **25**, L27.
[20] BRUNET, M., ANDERSSON, G., and LAGERWALL, S. T., 1987, *Molec. Crystals liq. Crystals*, **152**, 467.
[21] KONDO, K., KITAMURA, T., and MUKOH, A., 1987, *Abst. 13th Int. Liq. Cryst. Conf.* (Freiburg), FE47.
[22] SHINGU, T., TSUCHIYA, T., OUCHI, Y., TAKEZOE, H., and FUKUDA, A., 1986, *Jap. J. appl. Phys.*, **25**, L206.
[23] HIJI, N., OUCHI, Y., TAKEZOE, H., and FUKUDA, A., 1988, *Jap. J. appl. Phys.*, **27**, 8.
[24] GRINSTEIN, G., and PELCOVITS, R. A., 1982, *Phys. Rev.* A **26**, 2196.
[25] CHEN, J.-H., and LUBENSKY, T. C., 1976, *Phys. Rev.* A **14**, 1202.
[26] ROSENBLATT, CH. S., PINDAK, R., CLARK, N. A., and MEYER, R. B., 1977, *J. Phys., Paris*, **38**, 1105.
[27] PEREZ, A., BRUNET, M., and PARODI, O., 1981, *J. Phys., Paris*, **42**, 1559.
[28] KONDO, K., SATO, Y., MIYASATO, K., TAKEZOE, H., FUKUDA, A., KUZE, E., FLATISCHLER, K., and SKARP, K., 1983, *Jap. J. appl. Phys.*, **22**, L13.
[29] HIJI, N., CHANDANI, A. D. L., NISHIYAMA, S., OUCHI, Y., TAKEZOE, H., and FUKUDA, A., 1988, *Ferroelectrics*, **85**, 487 (*Proc. 1st Int. Symp. on Ferroelectric Liq. Cryst.* (Bordeaux-Arcachon, 1987)).
[30] HIJI, N., OUCHI, Y., TAKEZOE, H., and FUKUDA, A., 1988, *Jap. J. appl. Phys.*, **27**, L1.
[31] CLARK, N. A., and RIEKER, T. P., 1988, *Phys. Rev.* A (*Rapid Commun.*), **37**, 1053.
[32] OUCHI, Y., TAKANO, H., TAKEZOE, H., and FUKUDA, A., 1988, *Jap. J. appl. Phys.*, **27**, 1.
[33] ISHIKAWA, K., TAKEZOE, H., and FUKUDA, A., 1989, *Proc. 3rd Asia Pacific Physics Conference* (Singapore, 1988) edited by C. N. Yang, Y. W. Chan, K. Young and F. Leung (World Scientific) (in the press).
[34] ISHIKAWA, K., UEMURA, T., TAKEZOE, H., and FUKUDA, A., 1984, *Jap. J. appl. Phys.*, **23**, L666.
[35] BRUNET, M., and WILLIAM, CL., 1978, *Annls Phys.* (*Paris*), **3**, 237.
[36] BRUNET, M., and ISAERT, N., 1988, *Ferroelectrics*, **84**, 25 (*Proc. 1st Int. Symp. on Ferroelectric Liq. Cryst.* (Bordeaux-Arcachon, 1987)).
[37] PAVEL, J., 1984, *J. Phys., Paris*, **45**, 137.

[38] TSUCHIYA, T., OUCHI, Y., ISHIKAWA, K., TAKEZOE, H., FUKUDA, A., KONDO, K., ERA, S., and MUKOH, A., 1985, *Jap. J. appl. Phys.*, **24**, Suppl. 24–2, 896 (*Proc. 6th Int. Meeting on Ferroelectricity* (Kobe, 1985)).
[39] WULFF, G., 1901, *Z. Kristallogr.*, **34**, 449; OOKAWA, A., 1977, *Crystal Growth* (Syokabo), p. 163 [in Japanese].
[40] UEMURA, T., OHBA, N., WAKITA, N., OHNISHI, H., and OTA, I., 1986, *Japan Display '86* (*Proc. 6th Int. Display Research Conf.* (Tokyo, 1986)), 12.3, p. 464.
[41] BOS, P., and KOEHLER, R., 1988, *Ferroelectrics*, **85**, 403 (*Proc. 1st Int. Symp. on Ferroelectric Liq. Cryst.* (Bordeaux-Arcachon, 1987)).
[42] BOWRY, C., CLARK, M. G., MOSLEY, A., and NICHOLAS, B. M., 1987, *Proc. Eurodisplay '87* (London, 1987), C. 61, p. 33.
[43] SHIMIZU, K., and HIROSHIMA, K., 1988, *Extended Abst. 34th Spring Meeting of Jap. Soc. Appl. Phys. and Related Societies* (Tokyo), No. 3, p. 616, 30p-D-9.
[44] GOODMAN, L. A., MCGINN, J. T., ANDERSON, C. H., and DIGERONIMO, F., 1977, *I.E.E.E. Trans. electron Devices*, **24**, 795.
[45] MARTINOT-LAGARDE, PH., DUKE, R., and DURAND, G., 1981, *Molec. Crystals liq. Crystals*, **75**, 249.
[46] GOODBY, J. W., and CHIN, E., 1986, *J. Am. chem. Soc.*, **108**, 4736.
[47] ISHIKAWA, K., HASHIMOTO, K., TAKEZOE, H., FUKUDA, A., and KUZE, E., 1984, *Jap. J. appl. Phys.*, **23**, L211.
[48] HATANO, T., YAMAMOTO, K., TAKEZOE, H., and FUKUDA, A., 1986, *Jap. J. appl. Phys.* **25**, 1762.
[49] SATO, Y., TANAKA, T., NAGATA, M., TAKESHITA, H., and MOROZUMI, S., 1986, *Japan Display '86* (*Proc. 6th Int. Display Research Conf.* (Tokyo, 1986)), P2.13, p. 348.
[50] GAROFF, S., and MEYER, R. B., 1979, *Phys. Rev.* A, **19**, 338.
[51] TAKEZOE, H., FURUHATA, K., NAKAGIRI, T., FUKUDA, A., and KUZE, E., 1978, *Jap. J. appl. Phys.*, **17**, 1219.
[52] NISHIYAMA, S., OUCHI, Y., TAKEZOE, H., and FUKUDA, A., 1987, *Jap. J. appl. Phys.*, **26**, L1787.
[53] ANDERSSON, G., DAHL, I., KELLER, P., KUCZYNSKI, W., LAGERWALL, S. T., SKARP, K., and STEBLER, B., 1987, *Appl. Phys. Lett.*, **51**, 31.
[54] BAHR, CH., and HEPPKE, G., 1987, *Liq. Crystals*, **2**, 825.
[55] CHANDANI, A. D. L., OUCHI, Y., TAKEZOE, H., and FUKUDA, A., 1989, *Dynamic Behavior of Macromolecules, Colloids, Liquid Crystals and Biological Systems by Optical and Electro-Optical Methods* (*Proc. Int. Symp. ELECTROPTO 88* (Tokyo, 1988)), edited by H. Watanabe (Hirokawa Publishing Company), p. 399.
[56] OUCHI, Y., TAKEZOE, H., FUKUDA, A., KONDO, K., KITAMURA, T., YOKOKURA, H., and MUKOH, A., 1988, *Jap. J. appl. Phys.*, **27**, L733.
[57] CHANDANI, A. D. L., HAGIWARA, T., SUZUKI, Y., OUCHI, Y., TAKEZOE, H., and FUKUDA, A., 1988, *Jap. J. appl. Phys.*, **27**, L729.